Composites Part B 273 (2024) 111211

Contents lists available at ScienceDirect

Composites Part B

journal homepage: www.elsevier.com/locate/compositesb

An alternative method to evaluate the micromechanics tensile strength properties of natural fiber strand reinforced polyolefin composites. The case of hemp strand-reinforced polypropylene

F.X. Espinach [a,b,*], F. Vilaseca [c], Q. Tarrés [a,b,d], M. Delgado-Aguilar [a,b,d], R.J. Aguado [a,b], P. Mutjé [a,b]

[a] LEPAMAP-PRODIS Research Group, Dept. of Chemical and Agricultural Engineering and Agrifood Technology, Business Management and Product Design, University of Girona, C/Maria Aurèlia Capmany 61, 17003, Girona, Spain
[b] Dept. of Organization, Business Management and Product Design, University of Girona, C/Maria Aurèlia Capmany 61, 17003, Girona, Spain
[c] Advanced Biomaterials and Nanotechnology, Dept. of Chemical and Agricultural Engineering and Agrifood Technology, University of Girona, C/Maria Aurèlia Capmany 61, 17003, Girona, Spain
[d] Serra Húnter Programme, Via Laietana, 2, Barcelona, Spain

ARTICLE INFO

Handling Editor: Prof. Ole Thomsen

Keywords:
Natural fibers
Biocomposites
Micromechanics
Interfacial shear strength
Intrinsic tensile strength

ABSTRACT

Micromechanics models allow the prediction of a composite material's properties by adding their phases' contributions to such properties. The models can be used to obtain the intrinsic properties of the reinforcements because are difficult to obtain experimentally. This paper explores a simplified model to obtain the intrinsic strength of natural fibers. This model allows obtaining the value directly from the experimental strength of a composite and the matrix. Other models like the Kelly and Tyson equation have three unknowns, needing the use of mathematical methods to obtain a solution, and the obtained solution sometimes deviates from the expected values for natural fiber-reinforced composites. The proposed equation has been able to evaluate the intrinsic strength of hemp fibers as polypropylene composites at a mean value of 600 MPa. This value agrees with the literature. The proposed method simplifies the obtention of the intrinsic tensile strengths of natural fiber reinforcements and does not need morphologic properties of such reinforcements to obtain a solution, decreasing the costs in time and equipment in comparison to usual models like Kelly and Tyson's. furthermore, the obtained results are like those obtained with other micromechanics approaches and reveal the same information about the intrinsic tensile strength of the reinforcements and the strength of the interface.

1. Introduction

The tensile strength of a composite can be experimentally tested or predicted by using micromechanics models reducing the time needed to obtain a value by experimentation [1,2]. The use and costs due to such experimentation add more information about the expected behavior of the materials [2,3]. Certainly, there will be a difference between experimental and theoretical data, but if the model's limitations and assumptions are well-known these differences can be limited [4]. Nevertheless, as the authors will show in the revision of the micromechanics models commonly used for semi-oriented short fiber reinforced composites, the information needed to obtain the intrinsic properties of reinforcement include the tensile strength of the composite, the contribution of the matrix, the volume fractions of the phases and the evaluation of the morphology of the reinforcements. Evaluating the morphology of the reinforcements involves extracting such reinforcements from the matrix, usually using a soxhlet apparatus, and then the use of an analyzer. This increases the cost of the evaluation in time and equipment. The authors present a model that allows the evaluation of the intrinsic strength of the reinforcements without morphologic evaluation of the reinforcements.

The literature shows that the tensile strength of semi-oriented short fiber reinforced composites can be modeled with a modified rule of mixtures (mRoM) for the tensile strength [5–7]. The following notation will be used for the present work:

* Corresponding author. LEPAMAP-PRODIS Research Group, Dept. of Chemical and Agricultural Engineering and Agrifood Technology, Business Management and Product Design, University of Girona, C/Maria Aurèlia Capmany 61, 17003, Girona, Spain.
E-mail address: francisco.espinach@udg.edu (F.X. Espinach).

https://doi.org/10.1016/j.compositesb.2024.111211
Received 17 August 2023; Received in revised form 4 December 2023; Accepted 8 January 2024
Available online 12 January 2024

$$\sigma_t^C = f_c \sigma_t^F V^F + \sigma_t^{M*} V^M \quad (1)$$

In the equation σ_t^C, σ_t^F, and σ_t^{M*} are the tensile strength of the composite, the intrinsic tensile strength of the reinforcement, and the contribution of the matrix to the tensile strength of the composite [8]. Here some authors use the ultimate strength of the polymer while others use the stress corresponding to the strain at the break of the matrix in the stress-strain curve of the matrix [8,9]. When a stiff phase, like a natural fiber, is added to a tough matrix, the strain at the break of the resulting composite material tends to decrease noticeably. This effect is positively correlated with the percentage of reinforcement and negatively correlated with the strength of the interface between the reinforcement and the matrix [2,8,10]. In the case of natural fiber-reinforced composites, the literature shows a high decrease in the strain at the break of such composites compared to the matrix [11,12]. Hence, the authors will use the stress-strain curve of the polymer to evaluate its contribution to the tensile strength of the matrix. Returning to equation (1), V^F and V^M are the reinforcement and matrix volume fractions. It is common to assume that the composite has null porosity and then $V^M = 1 - V^F$. This assumption will be made for all the evaluated composites. Finally, f_c is a coupling factor that equalizes the contribution of the reinforcements by accounting for the impact of the strength of the interface, the mean length of the reinforcements, and its mean orientation regarding the tensile load [9,13]. Thus, the coupling factor can be found as the multiplication of an orientation factor (χ_1)by a length and interface factor (χ_2) and $f_c = \chi_1 \chi_2$ [9].

Thus, the mRoM includes all the factors that impact the final tensile strength of a composite. The mechanical properties of the phases (σ_t^C, σ_t^F and σ_t^{M*}). The percentage of the phases (V^F and V^M). The strength of the interface between the matrix and the reinforcement (χ_2). The morphology of the reinforcements (χ_2), mainly their mean length and diameter. The orientation of the reinforcements regarding the loads (χ_1).

All the previous factors can be evaluated experimentally, but some are more difficult to evaluate than others. The tensile strength of the composite and the matrix are evaluated during the tensile test and their strain at the break. The contribution of the matrix can be obtained from the stress-strain curves of the matrix, also a result of its tensile test. The volume fractions of the reinforcements and the matrix can be computed from their weight percentage and densities using equation (1) presented in the materials and methods section and then assuming no porosity to obtain the matrix volume fraction. The previous values are easily obtainable from the experimental data.

The intrinsic strength of the reinforcing fibers can be obtained experimentally or by micromechanics modeling [9,14]. The experimental evaluation involves using standards like ASTM D-3822 or similar. This standard calls for testing at least 20 fiber specimens at 10 mm gage length or greater and evaluating the diameter of the specimen. In the case of man-made fibers, such reinforcements are usually cylinders, but natural fibers show more complex shapes that can include lumens [15]. Moreover, the width of natural fibers can vary significantly and the area of the section under tensile can be over or under-estimated [16]. Besides, natural fibers are difficult to individualize and are commonly found in the shape of fiber bundles [17,18]. Thus, the experimental evaluation of the tensile strength of natural fibers commonly returns values with high scatter [19]. Furthermore, to evaluate the tensile strength of natural fibers experimentally, some authors advise evaluating their Weibull strength due to the fragile nature of such fibers [20–23]. On the other hand, micromechanics models like Kelly and Tyson's modified equation offer a way to evaluate the intrinsic strength of the reinforcement, the strength of the interface between the matrix and the reinforcement, and the orientation factor [24]. The equation is an evolution of the mRoM that differentiates the contribution of the fibers between subcritical and supercritical fiber contributions: $\sigma_t^C = \chi_1(X + Y) + Z$, being X, Y, and Z the contributions of the subcritical, supercritical fibers, and the matrix to the tensile strength of the composite. The critical length (L_c) is defined by the following equation [25]:

$$L_c = \frac{d_F \sigma_t^F}{2\tau} \quad (2)$$

In the equation, d_F, σ_t^F, and τ are the mean diameter of the reinforcements, the intrinsic strength of the reinforcements, and the interfacial shear strength or the strength of the interface, respectively. Supercritical fibers, with a length superior to the critical length, will be able to receive shear strengths from the matrix in their surface and accumulate enough load to reach their intrinsic tensile strength and break. Subcritical fibers will not be able to accumulate enough loads to break and will not break. Kelly and Tyson's modified equation has the following notation:

$$X = \sum_{l=0}^{l=Lc} \left[\frac{\tau \cdot l \cdot V_l^F}{d_F} \right]. \quad (3)$$

$$Y = \sum_{l=Lc}^{\infty} \left[\sigma_t^F \cdot V_l^F \cdot \left(1 - \frac{\sigma_t^F \cdot d_F}{4 \cdot \tau \cdot l} \right) \right] \quad (4)$$

$$Z = V^M \cdot \sigma_t^{m*}. \quad (5)$$

In the equations, l, and is the length of reinforcing fibers that have d_F as mean diameter and V_l^F as partial volume fraction. The sum of all fiber partial volume fractions equals V^F.

If the tensile strength of the composite, the length distribution of the fibers, and its mean diameter are known, the equation still has four unknowns, the intrinsic strength of the reinforcement, the orientation factor, the interfacial shear strength, and the critical length.

Fortunately, Bowyer and Bader developed a methodology to solve the equation. The solution is based on the assumption that the phases have an elastic region in the stress-strain curve. Then, the contribution of the reinforcements instead of σ_t^F will be $E_t^F \cdot \epsilon_t^C$ [26]. The method allows the evaluation of the interfacial shear strength, the orientation factor, and the critical length by numerical methods. Once these factors are known, Kelly and Tyson equation can be used to obtain the intrinsic tensile strength of the reinforcement. This methodology is fully described in the literature. The solution proposed by Bowyer and Bader has been used by some researchers and obtained reasonable results [27–30]. Nonetheless, the method is highly sensitive to minimal changes in the input data and on some occasions can return unreasonable results [31]. On the other hand, Kelly and Tyson's equation is very robust when reasonable data is used for its solution.

Natural fiber-reinforced composites have been of interest to the scientific community for a long period [32–34]. The opportunity to replace mineral reinforcements with natural fibers increases, priory, the value chain of the natural fiber producer, and the sustainability of the composite materials, but a life cycle analysis of any artifact produced with the composite is needed to sustain such an assertion [35,36]. Natural fibers are more lightweight, less abrasive, and less harmful than glass fibers, increasing the interest in natural fiber-based composites [32,37]. However, the properties of natural fibers are not as regular as those of man-made fibers and show noticeable scatters, being impacted by the region where are harvested and the climate [33]. Besides, natural fiber strength is mainly due to their cellulose content, and cellulose degrades at 200 °C, limiting the available matrices [38]. Polyolefin like high-density polyethylene (HDPE) and polypropylene (PP) can be mold injected below 200 °C and are appropriate for being reinforced with natural fibers [39–42]. Furthermore, PP and HDPE are commodity materials in the industry and their glass fiber composites are also common. Therefore, the evaluation of the intrinsic properties of natural fibers is important to preview the theoretical properties of their composites. These composites are of interest to the industry and have been used for automotive and construction purposes [43–47]. The

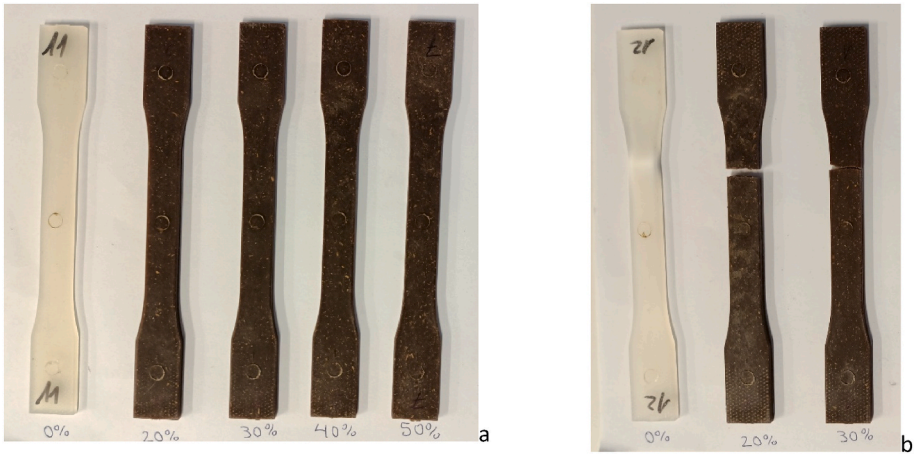

Fig. 1. matrix and composite standard specimens, a: matrix and 20 to 50 wt% HF composites with 6 wt% of MAPP, b: matrix and 20 and 30 wt% HF tested specimens.

authors choose hemp fibers as reinforcement of PP because such fibers and matrix are very well characterized in the literature and the composites show properties similar to glass fiber reinforced materials [17,44,48–51].

The author's research includes the evaluation of the intrinsic tensile strength of natural fibers as polymeric matrix reinforcement, and in some cases, this has been difficult due to the impossibility of obtaining sensible solutions from Bowyer and Bader's methodology. In this work, the authors present a methodology that can be used to obtain the micromechanics tensile properties of natural strand-reinforced polymers. The solution is based on a modified Hirsch equation devoted to the tensile strength of a composite reinforced with semi-aligned short fibers. To verify the results the authors have used the preliminary data obtained from the use of the Kelly and Tyson equation and Bowyer and Bader methodology for hemp fiber-reinforced polypropylene composites. This method has the assumption, based on the literature, that the orientation factor has a 0.3 value. The obtained results are similar to those obtained with the Kelly and Tyson equation and Bowyer and Bader methodology and are more easily obtained and less sensitive to variations of the experimental data than the Bowyer and Bader methodology. Moreover, the proposed methodology allows for obtaining sensible results without morphologic evaluation of the mean diameter and length distribution of the reinforcements required by the Kelly and Tyson equation.

2. Materials and methods

2.1. Materials

Composite materials used to evaluate the micromechanics models were made of two phases. The continuous phase was a polypropylene (PP) matrix ISPLEN® 090 G2M by Repsol Química S.A. (Tarragona, Spain). The matrix has a density of 0.905 g/cm^3. This matrix was gently provided by the manufacturer. The discrete phase or reinforcement was untreated hemp strands (HF) provided by Agrofibra S.L. (Puigreig, Spain). These strands were received with lengths between 20 and 30 cm and a 1.480 g/cm^3 density. A coupling agent based on maleic acid-grafted polypropylene (MAPP) was used to increase the strength of the interface.

A modified maleic anhydride-grafted polypropylene (MAPP) coupling agent was used: Epolene® G3015 from Eastman (Rotterdam, The Netherlands). This is a medium acid number (15 mg KOH/g) and molecular weight (24800 Da) coupling agent.

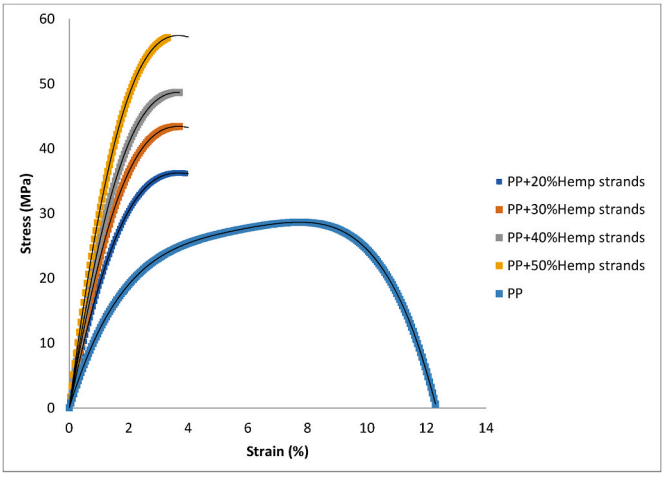

Fig. 2. Stress-strain curves of the hemp strand reinforced PP composites and the PP matrix.

2.2. Methods

2.2.1. Composite preparation and characterization

Before mixing hemp strands were chopped at a nominal length of 5 mm in a blade mill. Next, the strands were dried in an oven for 24 h at 80 °C. The phases were mixed in a heated roll mixer for 10 min at 108 ± 5 °C. Composites adding 20, 30, 40, and 50 wt% HF contents. These composites were produced with 0, 2, 4, 6, and 8 wt% MAPP contents. MAPP content was evaluated regarding HF content. Thus, twenty different composite materials were prepared. The resulting blends were pelletized in a blade mill. These pellets were dried in a stove for 24 h at 85 °C before mold injection.

Dog bone specimens in agreement with ASTM D638 were obtained in an injection molding equipment Meteor 40 by Mateu & Solé (Barcelona, Spain) (Fig. 1a). The machine has three main heating zones and is operated at 175, 180, and 190 °C. The two first heating zones correspond to the barrel and the last to the nozzle. The steel injection mold was cooled at 70 °C. Filling and maintaining pressures were 117.7 and 24.5 bar, respectively. The mold injection cycle lasted 45 s. The specimens were conditioned at 23 °C and 50 % relative humidity for 48 h before tensile testing. At least 10 specimens of any of the composites were obtained.

The tensile test was carried out in agreement with ASTM D638. Specimens were attached to the clamps of an Instron® 1122 Universal

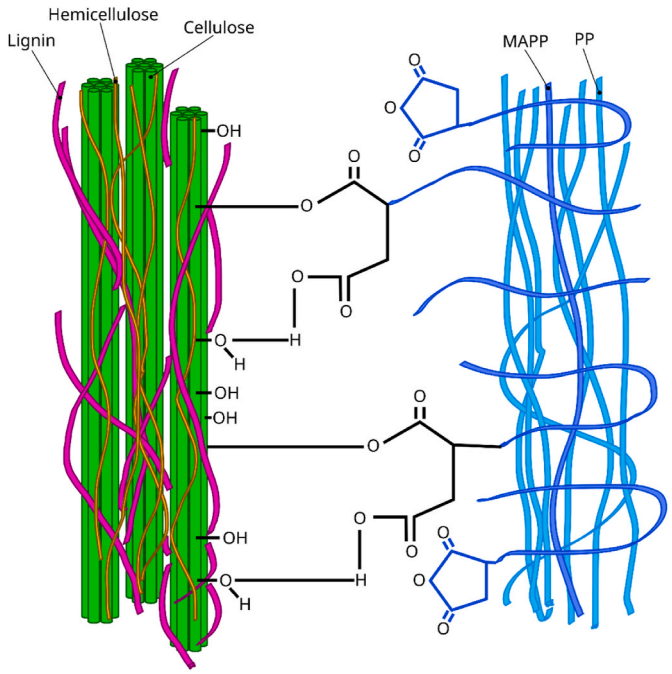

Fig. 3. Reaction of MAPP maleic anhydride with the hydroxyl groups of cellulose in natural fiber surfaces.

testing machine (Barcelona, Spain). The test was operated at 2 mm/min, and the measurements were obtained from the 5 kN load cells equipped by the machine. At least 5 valid tests for any of the composites were obtained. Fig. 1b shows the matrix and the 20 and 30 wt% tested specimens.

ANOVA of the experimental results was performed in R® at a 95 % confidence rate.

2.3. Evaluation of the contribution of the matrix

The authors made a mean stress-strain curve from the tensile tests (Fig. 2).

From the curve of the matrix, the authors obtained a curve fitting:

$$\sigma_t^{M*} = -0.0159\left(\varepsilon_t^C\right)^4 + 0.3712\left(\varepsilon_t^C\right)^3 - 3.3674\left(\varepsilon_t^C\right)^2 + 14.895\varepsilon_t^C + 0.0493 \quad (6)$$

This equation will be used in all the models that input matrix contribution to the tensile strength. In the equation, ε_t^C is the strain at the break of the composite. Composite materials are more fragile than the matrix and break at strain lower than such matrix. Thus, the contribution of the matrix to the strength of the composite is considered as the stress of the matrix at the strain at the break of the composite. Thus, the curve fitting equation is used to obtain the contributions of the matrix by imputing the strains at the break of the composites.

2.4. Volume fractions

Reinforcement volume fractions were obtained from the following equation:

$$V^F = \frac{w^F \cdot \rho^F}{w^m \cdot \rho^F - w^F \cdot \rho^m} \quad (7)$$

In the equation, ρ^F, w^F and ρ^m, w^m are the densities and mass fractions of the reinforcement and the matrix, respectively [52].

Table 1
Tensile strength of hemp fiber reinforced polypropylene composites against reinforcement and coupling agent contents.

	0 wt% MAPE	2 wt% MAPE	4 wt% MAPE	6 wt% MAPE	8 wt% MAPE
20 wt% HF	29.5 ± 0.6^{ab}	30.7 ± 0.4^{bc}	33.3 ± 0.4^{cd}	34.7 ± 0.4^{de}	36.3 ± 0.3^{e}
30 wt% HF	32.6 ± 0.4^{cd}	37.2 ± 1.0^{ef}	43.4 ± 0.8^{h}	42.4 ± 1.2^{gh}	39.8 ± 0.6^{fg}
40 wt% HF	32.8 ± 1.2^{cd}	44.2 ± 1.7^{hi}	48.8 ± 1.6^{ik}	48.3 ± 1.2^{j}	46.4 ± 1.4^{ij}
50 wt% HF	34.5 ± 1.5^{de}	51.6 ± 2.3^{k}	57.1 ± 2.4^{l}	55.9 ± 0.7^{l}	51.4 ± 1.1^{k}

Different letters a, b, c, d, e, f, g, h, i, j, k, and l represent the statistical difference (ANOVA, $p < 0.05$) between the properties of the materials.

3. Results and discussion

3.1. Experimental results

In the introduction section, it is said that the percentages of the phases and the strength of the interface between such phases were among the factors that impact the tensile strength of a composite. Natural fibers are hydrophilic and polymers like PP are hydrophobic [29,53,54]. Then, these phases show poor compatibility, and untreated fibers are expected to show weak interfaces. This is the reason why the researchers added a coupling agent to the composites, to promote the creation of a chemical bond between the surface of the fibers and the maleic acid of MAPP. The hydroxyl groups of the cellulose present in the natural fiber surface react with the anhydride of maleic acid (Fig. 3). On the other hand, PP chains of MAPP entangle with the matrix.

MAPP reacts with the cellulose in the fiber surface by creating hydrogen bonds and ester bonds with the hydroxyl groups. On the other hand, PP chains of MAPP co-crystallize and entangle with the matrix [37]. Table 1 shows the experimental results of the tensile tests of hemp strand-reinforced polypropylene composites.

The results show the impact of adding the coupling agent to the composites. In all the cases the tensile strength of the materials increases noticeably with the presence of MAPP up to 4 wt%. Then some of the composites show a decrease in their tensile strength.

What is more relevant, despite the chemical incompatibility between HF and PP, composite materials without coupling agents increased the tensile strength of the PP matrix (27.6 ± 0.5 MPa). This can be due to the mechanical anchorage of the fibers to the matrix. Fig. 4 shows a micrograph of the surface of the fibers and the fiber-matrix interface for a coupled composite.

Fig. 4A shows the surface of a fiber bundle, with some rugosity that can enhance the creation of mechanical anchoring. Moreover, the matrix can percolate through the spaces inside the fiber bundle. Nonetheless, this micrograph was taken from the raw material before mechanical treatment, thus, hemp strands used to prepare the composites were more individualized. The morphological analysis of the stands extracted from the composites with 20, 30, 40, and 50 wt% HF returned mean diameters of 30.8, 33.0, 30.8, and 32.0 μm, respectively. Fig. 4A also shows an individualized fiber with a diameter lower than the one obtained in the morphological analysis. Thus, HF used to obtain the composites was more individualized than the raw material but not fully individualized. The authors hypothesize the presence of fiber bundles with 2–5 fibers. Fig. 4B shows the interface between a fiber and the matrix. Here the rugous surface of the fiber can be observed and the interfacial zone shows contact between the fiber and the matrix, typical of uncoupled composites [55,56].

Fig. 5A shows the evolution of the tensile strength of the composites against MAPP content.

The figure shows how the tensile strength of the composites with HF contents 30 wt% or higher increases noticeably when the MAPP

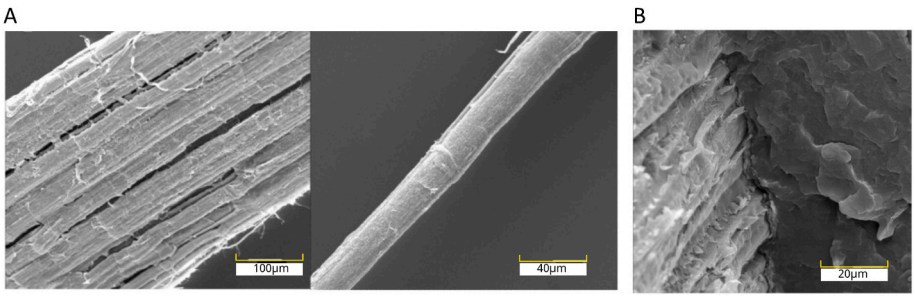

Fig. 4. SEM micrographs of hemp strands; A: fibers bundle and individualized fiber; B: the interface between a fiber and the matrix in a coupled composite.

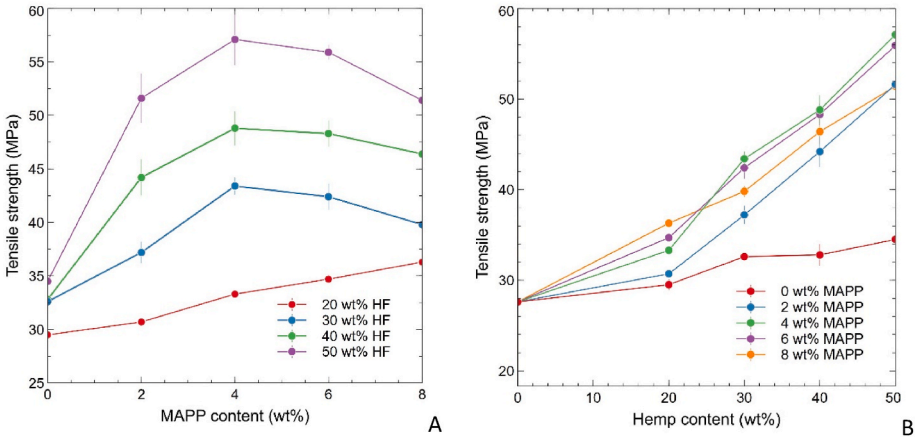

Fig. 5. Evolution of the tensile strength of hemp strand reinforced polypropylene composites; A, against coupling agent content, B, against hemp strand content.

percentage increases from 0 to 2 wt%. Then, the effect of MAPP decreases for the composites with HF contents 30 wt% or superior, and increases for the rest of the composites, as shown by the slope of the corresponding curves. In the case of the composite that added 20 wt% of HF, its tensile strength continues growing almost linearly for increasing amounts of MAPP. The other composites show a stabilization of the effect of the MAPP and even a decrease in their tensile strengths. This effect is more noticeable for 8 wt% MAPP contents. Thus, there are two different behaviors of the composite when MAPP was added. On the one hand, the composites with HF contents 30 wt% or higher, with a tensile strength that increases for MAPP contents up to 4 wt% and then stabilizes or decreases. This behavior has been reported in the literature and is linked to self-entanglement and reactions of MAPP instead of reacting with the hydroxyl groups of the cellulose. Anova analysis shows that there are no statistical differences between the impact of 4 and 6 wt% MAPP contents in the tensile properties of composites with 30, 40, and 50 HF wt%. However, being the mean tensile strength of the polymers with 4 wt% of MAPP the highest and to minimize the use of reactants, the authors consider that 4 wt% of MAPP guarantees the highest tensile strengths and thus provides the strongest interfaces.

The case of the composites adding 20 wt% of HF shows a different behavior. The tensile strength of these composites increases almost linearly up to 8 wt% MAPP contents. Possibly, higher tensile strengths can be achieved by increasing the percentage of MAPP, but this is out of the scope of the paper. The authors expect that the strongest interface for the tested composites at 20 wt% HF content will be found for 8 wt% MAPP contents. Fig. 5B shows the evolution of the tensile strength of the composites against HF content. The tensile strength of the composites increases with the percentage of HF despite MAPP content. Table 1 shows that the effect of NF content on the tensile strength of the composites is statistically relevant.

Information in Table 1 can be converted into a surface by plotting the points as a point cloud and obtaining the resulting surface. Then the lines corresponding to iso-strength can be obtained from such surface [48]. Fig. 6 shows the resulting surface.

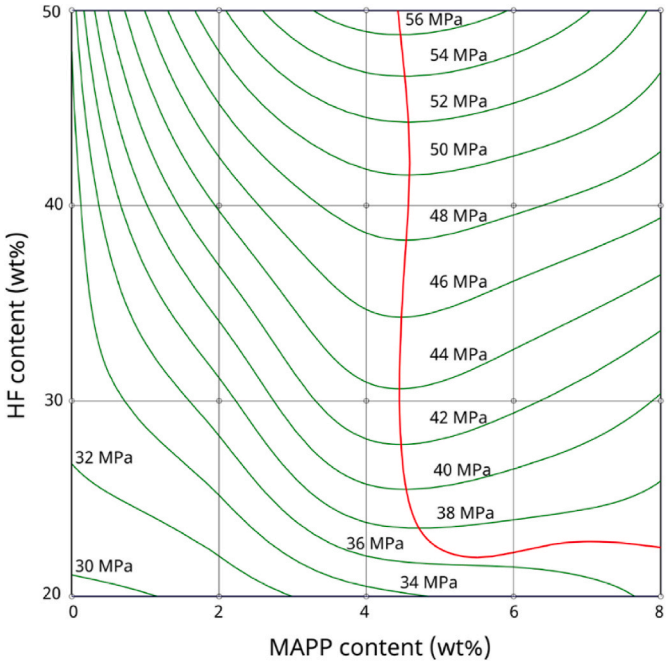

Fig. 6. Topographic map of a Surface obtained from the tensile strength of the composites mapped against hemp strand and MAPP contents.

The most notable result is the corroboration that the highest tensile experimental strengths are obtained with 4 wt% MAPP contents. The figure shows that theoretically higher tensile strengths can be obtained

Table 2
Experimental data used to obtain the intrinsic tensile strength of HF from the Kelly and Tyson equation, and coupling factors of the composites form the mRoM.

HF (wt %)	MAPP (wt %)	VF	σ_t^C	ε_t^C	σ_t^{m*}	σ_t^F	fc	fc
20	4	0.132	36.3	3.9	25.26	472	0.23	0.18
30	4	0.206	43.4	3.7	24.88	528	0.22	0.19
40	4	0.288	48.8	3.5	24.46	617	0.18	0.18
50	8	0.378	57.1	3.3	23.98	607	0.18	0.18

Table 3
Coupling factors of hemp fiber-reinforced polypropylene composites against reinforcement and coupling agent contents obtained from a modified rule of mixtures with an intrinsic tensile strength of 617 MPa. The strain at the break of the composites is presented between the brackets and is used to obtain the contribution of the matrix.

	0 wt% MAPP	2 wt% MAPP	4 wt% MAPP	6 wt% MAPP	8 wt% MAPP
20 wt% HF	0.10 (3.4)	0.12 (3.3)	0.15 (3.6)	0.15 (4.0)	0.18 (3.9)
30 wt% HF	0.11 (3.1)	0.15 (3.1)	0.19 (3.7)	0.18 (3.5)	0.16 (3.4)
40 wt% HF	0.09 (2.9)	0.15 (3.3)	0.18 (3.5)	0.17 (3.5)	0.17 (3.3)
50 wt% HF	0.09 (2.8)	0.16 (3.1)	0.18 (3.3)	0.18 (3.2)	0.16 (3.0)

with MAPP dosages near 5 wt%. This is reflected by the red line that corresponds with the silhouette of the surface and shows the highest strength points.

3.2. Micromechanics

3.2.1. Using Kelly and Tyson's equation

In prior research, some of the authors determined the intrinsic tensile strength of HF by using Kelly and Tyson equations and the solution provided by Bowyer and Bader [29]. Table 2 shows such results for the composites that returned the highest tensile strengths.

The literature puts the intrinsic tensile strength of hemp strands between 550 and 900 MPa [57,58]. The obtained results are inside or near these values. The values obtained from the Kelly and Tyson equation, or any micromechanics model can be read as the exploitation of the strengthening capabilities of the reinforcement. Then the obtained value is not nominal and is a lower bound for the property. As an example, the intrinsic tensile strength of an HF as reinforcement for a composite adding 20 wt% of HF and 8 wt% of MAPP is $\geq$ 472 MPa. Then, the exploitation of such strengthening capabilities equals 472 MPa. Moreover, intrinsic tensile strength is positively correlated to fiber length, and such fiber length is negatively correlated to reinforcement content [59]. The rationale under these correlations is that the higher the reinforcement content the higher the attrition phenomena that the fibers are subjected to during mixing operations. This attrition causes fiber shortening. This shortening was observed for the HF-based composites, and the mean lengths for the fibers extracted from the 20, 30, 40, and 50 wt% HF-reinforced composites were 1277, 943, 819, and 785 μm, respectively. Then, the probability of finding an error in a fiber surface increases with the length of such fibers, and the literature shows such a relation [31]. Thus, obtaining higher intrinsic tensile strength for a composite at 50 wt% of HF than for the 30 and 20 wt% composites deviates from the commented rationale. This deviation is more visible when the coupling factor is evaluated using the mRoM (Equation (1)) in Table 2. The penultimate row of the table shows the theoretical coupling factors of the composites using the obtained intrinsic tensile strengths. The obtained results show coupling factors higher than 0.2 for the composites at 20 and 30 wt% HF contents. These values can be considered too high because the literature shows that coupling factor values between 0.18 and 0.20 correspond to strong to optimal interfaces for semi-oriented short fiber reinforced composites [13]. The cause for these values is underestimating the intrinsic tensile strength of the reinforcement. The last row of Table 2 shows the coupling factor values obtained supposing the same 617 MPa intrinsic tensile strength of HF for all the composites. The higher the intrinsic tensile strength the lower the coupling factor. Thus attending to the rationale that micromechanics models deliver lower bounds for the intrinsic tensile strength, the obtained coupling factors will be lower or equal to the values in Table 2. Table 3 shows the evolution of the coupling factor against HF and MAPP contents.

Table 4
Intrinsic tensile strength of hemp fiber obtained from the experimental results and with a 0.1 load transfer factor.

	0 wt% MAPP	2 wt% MAPP	4 wt% MAPP	6 wt% MAPP	8 wt% MAPP
20 wt% HF	204.1	303.8	435.4	476.2	**608.0**
30 wt% HF	230.8	436.9	**647.5**	624.2	515.0
40 wt% HF	139.4	440.9	**573.3**	556.6	513.7
50 wt% HF	108.4	452.6	**571.7**	550.7	458.0
Mean	170.7 ± 56.5	408.5 ± 70.1	557.0 ± 88.4	551.9 ± 62.2	523.0 ± 62.1

The values of the coupling factor show a similar evolution to the tensile strength of the polymers (Table 1). The composites that returned the highest coupling factors added 8 wt% of MAPP for the composite at 20 wt% HF content and 4 wt% of MAPP for the rest of the materials.

In summary, it was possible to obtain sensible values for the micromechanics factors of the tensile strength of HF as a PP composite. Nonetheless, as shown in the literature this is not always possible. Thus the authors propose a methodology that can provide the same micromechanics properties when the Kelly and Tyson equation cannot be solved.

3.2.2. Using the Hirsh equation

Hirsch mixed Reuss and Voigt models to evaluate the contribution of fibers parallel and perpendicular to the loads [60]. The equation is commonly used to model Young's modulus of composites but some authors defend that can be used to model the tensile strength of composites [9]. Its notation is as follows:

$$\sigma_t^C = \beta\left[\sigma_t^f V^F + \sigma_t^{M*} V^M\right] + (1\text{-}\beta)\frac{\sigma_t^f \sigma_t^{M*}}{\sigma_t^{M*} V^F + \sigma_t^f V^M} \quad (8)$$

The equation adds a load transfer factor (β) that evaluates the contributions of parallel and perpendicular fibers to the tensile strength of the composites. The literature establishes a value of 0.4 for the load transfer factor in the case of Young's modulus, but there is no consensus for its value when used to compute the tensile strength. Some authors provide the same 0.4 value and others 0.1 or 0.15 [9]. Authors using a value of 0.15 consider σ_t^{M*} as the tensile strength of the matrix and those using a 0.1 value consider σ_t^{M*} as the tensile stress of the matrix at the strain at the break of the composite [61–63]. Therefore, the authors will use a 0.1 value for β. Table 4 shows the intrinsic tensile strength of the composites obtained with the Hirsh equation.

Alike the case of the results obtained from the Kelly and Tyson equation (Table 2), the intrinsic tensile strengths of HF reflect the exploitation of their strengthening capabilities. Then, the higher the tensile strength of a composite, the higher such exploitation. The intrinsic value obtained for the composite at 20 wt% is lower than the obtained for the composite at 30 wt%, but looking at Fig. 5A it is possible that the coupling dosage for the 20 wt% composite can be increased and

Table 5
Coupling factors of hemp fiber-reinforced polypropylene composites against reinforcement and coupling agent contents obtained from a modified rule of mixtures with an intrinsic tensile strength of 647.5 MPa.

	0 wt% MAPP	2 wt% MAPP	4 wt% MAPP	6 wt% MAPP	8 wt% MAPP
20 wt% HF	0.10	0.12	0.14	0.15	0.17
30 wt% HF	0.10	0.14	0.18	0.17	0.15
40 wt% HF	0.09	0.15	0.17	0.17	0.16
50 wt% HF	0.08	0.15	0.17	0.17	0.15

Table 6
Length and interface factors of hemp fiber-reinforced polypropylene composites against reinforcement and coupling agent contents obtained from a 0.3 orientation factor and the coupling factors of the composites.

	0 wt% MAPP	2 wt% MAPP	4 wt% MAPP	6 wt% MAPP	8 wt% MAPP
20 wt% HF	0.33	0.39	0.46	0.49	0.56
30 wt% HF	0.35	0.46	0.59	0.57	0.51
40 wt% HF	0.30	0.48	0.56	0.55	0.52
50 wt% HF	0.28	0.50	0.57	0.56	0.50

thus its tensile strength.

The mean value for the maximum intrinsic strengths for all HF contents (data in bold font in Table 4) is 600.1 ± 35.8 MPa, not far from the 556 ± 68.7 MPa obtained from the Kelly and Tyson equation. Moreover, the highest values obtained with both methods are 617 and 647 MPa. These solutions are inside the values predicted in the literature.

The results obtained with the Hirsch equation reveal that the intrinsic tensile strength of HF will be ≥ 647.5 MPa. This value can be used to evaluate the corresponding coupling factor for the mRoM and compare the values with those obtained from the Kelly and Tyson equation (Table 3). Table 4 shows the obtained values.

The differences between the values in Tables 3 and 5 are always <0.01, Thus the coupling factors obtained from any of the methods, in the case of HF-reinforced PP composites, can be considered equivalent.

One of the micromechanics properties of the composites that can be obtained from Bowyer and Bader's solution is the orientation factor. The value of such a factor has been used by the authors to validate the obtained solutions. The mean orientation of the fibers of a short fiber mold injected composite is highly determined by the properties of the composite, mainly its fluidity, the parameters used during mold injection, and the geometry of the mold. The authors have found that, with their equipment, the orientation factor shows always values around 0.3 ± 0.5 [20,29,64]. Then, when Bowyer and Bader's solution returns orientation factors out of this range, the authors do not accept the solution as plausible. Hence, the authors can fix the value of the orientation factor at 0.3. The authors advise the evaluation of the typical orientation factors of other researchers' equipment to apply the next steps of the methodology. Moreover, the orientation factor is linked to a mean orientation angle (α) by the following equation [29]:

$$\chi_1 = cos^4(\alpha) \tag{9}$$

Then, the mean orientation angle for a 0.3 ± 0.5 orientation factor is 42.3 ± 2.7°. Then, taking into account that $f_c = \chi_1\chi_2$, the length and interface factor (χ_2) can be obtained from the value of the orientation factor in Table 5. Table 6 shows the obtained length and interface factors.

Table 7
Critical lengths (μm) of hemp strands obtained from Fu and Lauke equations.

	L_F (μm)	0 wt% MAPP	2 wt% MAPP	4 wt% MAPP	6 wt% MAPP	8 wt% MAPP
20 wt % HF	1277	1933.3[a]	1657.0[a]	1378.2[a]	1297.2[a]	**1122.5[b]**
30 wt % HF	943	1349.8[a]	1015.6[a]	**771.7[b]**	803.0[b]	916.9[b]
40 wt % HF	819	1386.1[a]	844.7[a]	**719.1[b]**	733.7[b]	779.5[b]
50 wt % HF	785	1406.6[a]	778.7[b]	**668.1[b]**	690.3[b]	779.0[b]

Table 8
Interfacial shear strength of hemp fiber reinforced polypropylene composites against reinforcement and coupling agent contents.

	d_F (μm)	σ_t^F (MPa)	0 wt% MAPP	2 wt% MAPP	4 wt% MAPP	6 wt% MAPP	8 wt% MAPP
20 wt % HF	30.8	608.0	5.61	6.16	7.14	7.22	**8.90**
30 wt % HF	33.0	647.5	8.94	11.05	**14.91**	14.26	12.29
40 wt % HF	30.8	573.3	7.81	10.97	**13.11**	12.81	11.98
50 wt % HF	32.0	571.7	8.24	12.37	**14.67**	14.14	12.36

Typical length and interface factors for coupled composites are around 0.5 ± 0.1 [29]. All the obtained values are inside this range. Uncoupled composites returned lower interface and length factors. These values can be used with Fu and Lauke equations for the length and interface factor to obtain a theoretical value for the critical length of HF for the composites [65]. Fu and Lauke's equations define two scenarios:

$$\chi_2 = \frac{L_F}{2L_C} \quad for \quad L_F \leq L_C \tag{10}$$

$$\chi_2 = 1 - \frac{L_C}{2L_F} \quad for \quad L_F \geq L_C \tag{11}$$

Table 7 shows the resulting critical lengths.

Different letters a and b correspond to the use of equation (10) (a) or equation (11) (b) to obtain the critical lengths.

All critical lengths were computed using equations (10) and (11), and then depending on the relation between L_F and L_C the corresponding value was chosen. As defined in equation (2), the stronger the interface the shorter the critical length. Then this equation can be used to obtain the interfacial shear strength of the composites. Table 8 shows the obtained values.

Bowyer and Bader's methodology uses the intrinsic tensile strength particular to the composite (Table 2). To compare the results, the authors have used the intrinsic tensile strength of HF for every composite. These intrinsic tensile strengths are lower bounds, thus, the interfacial shear strengths are also lower bounds. The literature shows that strong interfaces will return interfacial shear strength between von Mises and Tresca criteria [66]. These criteria are defined from the tensile strength

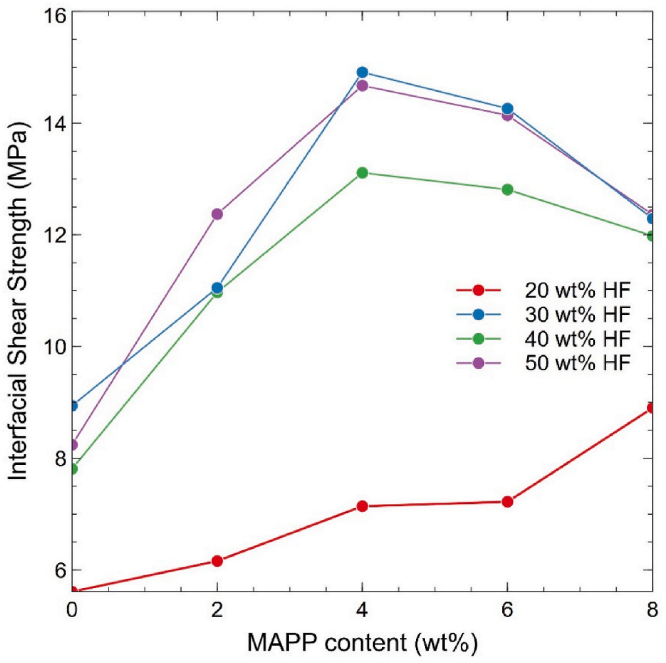

Fig. 7. Evolution of the interfacial shear strength of hemp strand reinforced polypropylene composites against coupling agent content.

of the matrix. Von Mises criteria announce that the interface can not be stronger than its weakest phase, and the shear strength of the matrix can be approximated by its tensile strength divided by the square root of 3. Tresca criteria divide the tensile strength of the matrix by half. Then, strong interfaces will return interfacial shear strengths in the range of 13.8–15.9 MPa. The interfacial shear strengths obtained using Bowyer and Bader solution for the 20, 30, 40, and 50 HF wt% composites were 14.85, 13.05, 14.25, and 15.6 MPa, respectively. These values are higher than those obtained with the proposed methodology, but the information is similar, returning strong interfaces for the composites, except for the composite with 20 wt% of HF. Fig. 7 shows the evolution of the interfacial shear strength against MAPP content.

The figure shows how the highest interfacial strengths coincided with the dosages of coupling agents defined to obtain the highest tensile strengths. The results show that although the obtained interfacial shear strengths are typical for strong interfaces, there is the possibility of obtaining composites with stronger interfaces and thus higher tensile strengths. The topological approach Fig. 6 announces that composites with MAPP contents between 4 and 5 wt% have the potential to achieve higher tensile strength. The figure shows that the composites at 20 wt% of HF did not reach a strong interface and possibly dosages higher than 8 wt% of MAPP are necessary to do so. The slope of the line between 6 and 8 wt% contents shows a noticeable increase in its slope.

Fig. 8 shows the scheme of the proposed methodology abe to obtain the intrinsic tensile strength of the composites, its coupling factor, and the interfacial shear strength of the interface.

4. Conclusions

Tensile micromechanics properties of hemp strand reinforced polypropylene composites obtained by mold injection have been obtained by a proposed methodology, based on a modified rule of mixtures and Hirsch's equation. The micromechanics properties are the intrinsic tensile strength of hemp strands, the interfacial shear strength, and the coupling factor. The proposed methodology assumes a 0.3 orientation factor.

The authors found that 4 wt% MAPP contents returned the highest tensile strengths for the composites. Using a modified rule of mixtures with the obtained values, the resulting coupling factors range from 0.18 to 0.19. The obtained intrinsic tensile strength of hemp strands reveals a lower bound value of 647.5 MPa. This value was obtained with Hirsch's equation and using a 0.1 load transfer factor. The intrinsic tensile strength of the reinforcement is positively correlated with the strength of the interface and the value obtained by using the Kelly and Tyson equation is 617 MPa, compatible with the result obtained from Hirsh's equation.

A topographic representation of the strengths of the composites against reinforcement and coupling agent contents can be used to

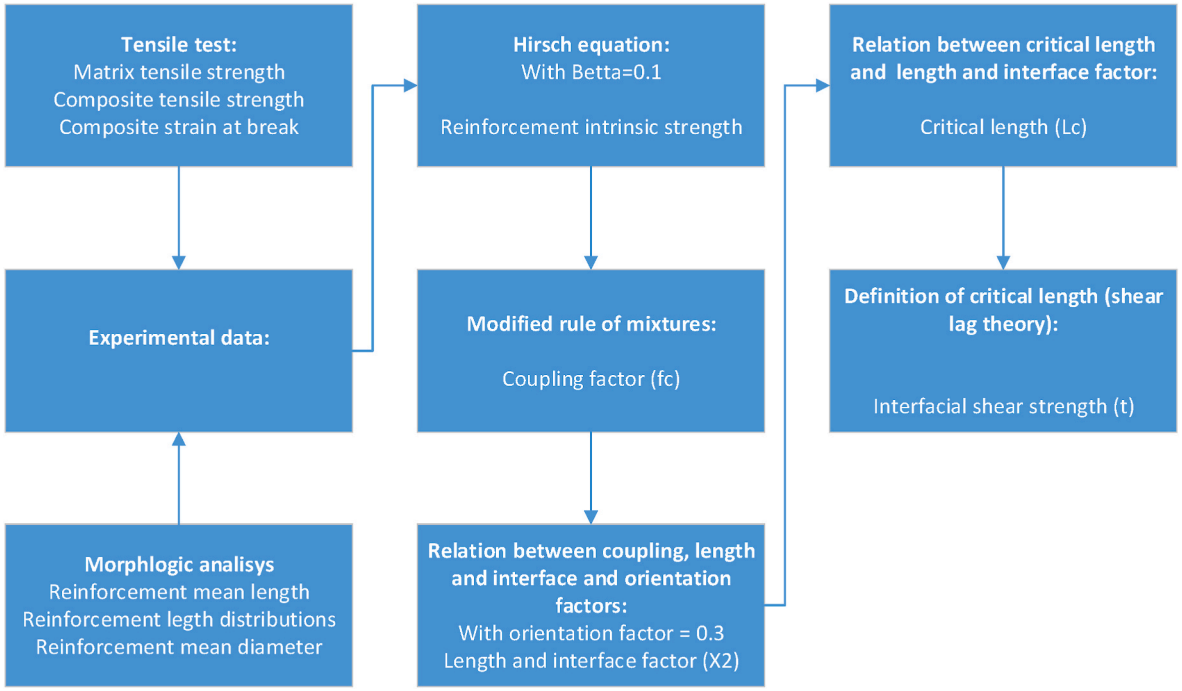

Fig. 8. Scheme of the proposed methodology to obtain the micromechanics tensile properties of semi-oriented short fiber reinforced composites.

further explore optimizations of the strength of the interface.

An integrated micromechanics methodology for the prediction of the tensile properties of semi-aligned short fiber-reinforced polymer composites has been developed and overcomes some limits that more usual micromechanics approaches, based on the solution to Kelly and Tyson's equation proposed by Bowyer and Bader have.

The proposed methodology is not dependent on the shape of the stress-strain curve of the matrix and the composites. Moreover, the methodology does not need a fiber length distribution and only a mean length of the reinforcements that can be obtained by optical microscopy instead of a morphologic analysis.

More work is needed to validate if the value of the load transfer factor is the same for different matrices and other natural fibers like wood fibers with different surface chemical compositions.

CRediT authorship contribution statement

F.X. Espinach: Conceptualization, Formal analysis, Methodology, Writing – original draft, Writing – review & editing. **F. Vilaseca:** Formal analysis, Writing – review & editing. **Q. Tarrés:** Formal analysis, Investigation, Writing – original draft. **M. Delgado-Aguilar:** Conceptualization, Investigation, Methodology, Validation, Writing – review & editing. **R.J. Aguado:** Investigation, Methodology, Writing – review & editing. **P. Mutjé:** Methodology, Supervision, Validation.

Declaration of competing interest

The authors declare the following financial interests/personal relationships which may be considered as potential competing interests:

F. X. Espinach reports financial support was provided by Universitat de Girona.

Data availability

Data will be made available on request.

References

[1] Konigsberger M, Lukacevic M, Fussl J. Multiscale micromechanics modeling of plant fibers: upscaling of stiffness and elastic limits from cellulose nanofibrils to technical fibers. Mater Struct 2023;56(1).

[2] Espinach FX, Julian F, Alcala M, Vilaseca F, Carrasco F, Mutje P. Effective tensile strength estimation of natural fibers through micromechanical models: the case of henequen fiber reinforced-PP composites. Polymers 2022;14(22).

[3] Sittner P, Novak V. Experiment feedbacks in micromechanics modeling of thermomechanical behaviors of SMA polycrystals. Scripta Mater 2004;51(4):321–6.

[4] Shah DU, Nag RK, Clifford MJ. Why do we observe significant differences between measured and 'back-calculated' properties of natural fibres? Cellulose 2016;23(3):1481–90.

[5] Esmaeili M, Zadhoush A, Javid KM. A new model to determine the tensile strength of short fiber-reinforced composites. In: 10th international Conference on Textile composites (TEXCOMP 10). Lille, FRANCE: Lille Grand Palais; 2010. 521-+.

[6] Rangaraj SS, Bhaduri SB. A modified rule-of-mixtures for prediction of tensile strengths of unidirectional fiber-reinforced composite-materials. J Mater Sci 1994;29(10):2795–800.

[7] Tham MW, Fazita MRN, Khalil H, Zuhudi NZM, Jaafar M, Rizal S, et al. Tensile properties prediction of natural fibre composites using rule of mixtures: a review. J Reinforc Plast Compos 2019;38(5):211–48.

[8] Tarrés Q, Melbø JK, Delgado-Aguilar M, Espinach F, Mutjé P, Chinga-Carrasco G. Micromechanics of tensile strength of thermo-mechanical pulp reinforced poly (lactic) acid biodegradable composites. J Nat Fibers 2022;19(15):9931–44.

[9] Yan J, Demirci E, Gleadall A. Are classical fibre composite models appropriate for material extrusion additive manufacturing? A thorough evaluation of analytical models. Addit Manuf 2023;62:103371.

[10] Mengesha Medibew T. A comprehensive review on the optimization of the fused deposition modeling process parameter for better tensile strength of PLA-printed parts. Adv Mater Sci Eng 2022:2022.

[11] Ramachandran A, Mavinkere Rangappa S, Kushvaha V, Khan A, Seingchin S, Dhakal HN. Modification of fibers and matrices in natural fiber reinforced polymer composites: a comprehensive review. Macromol Rapid Commun 2022;43(17):2100862.

[12] Jagadeesh P, Puttegowda M, Boonyasopon P, Rangappa SM, Khan A, Siengchin S. Recent developments and challenges in natural fiber composites: a review. Polym Compos 2022;43(5):2545–61.

[13] Tarrés Q, Oliver-Ortega H, Espinach FX, Mutjé P, Delgado-Aguilar M, Méndez JA. Determination of mean intrinsic flexural strength and coupling factor of natural fiber reinforcement in polylactic acid biocomposites. Polymers 2019;11(11):1736.

[14] Thomason J. On the application of Weibull analysis to experimentally determined single fibre strength distributions. Compos Sci Technol 2013;77:74–80.

[15] Liu K, Takagi H, Osugi R, Yang ZM. Effect of lumen size on the effective transverse thermal conductivity of unidirectional natural fiber composites. Compos Sci Technol 2012;72(5):633–9.

[16] Granda LA, Espinach FX, Mendez JA, Tresserras J, Delgado-Aguilar M, Mutje P. Semichemical fibres of Leucaena collinsii reinforced polypropylene composites: young's modulus analysis and fibre diameter effect on the stiffness. Compos Pt B-Eng. 2016;92:332–7.

[17] Lu C, Wang CH, Li CH, Tong JF, Sun YF. Structural and mechanical properties of hemp fibers: effect of progressive removal of hemicellulose and lignin. J Nat Fibers 2022;19(16):13985–94.

[18] Serra-Parareda F, Julian F, Espinosa E, Rodriguez A, Espinach FX, Vilaseca F. Feasibility of barley straw fibers as reinforcement in fully biobased polyethylene composites: macro and micro mechanics of the flexural strength. Molecules 2020;25(9).

[19] Sinha AK, Bhattacharya S, Narang HK. Abaca fibre reinforced polymer composites: a review. J Mater Sci 2021;56(7):4569–87.

[20] Seculi F, Espinach FX, Julián F, Delgado-Aguilar M, Mutjé P, Tarrés Q. Evaluation of the strength of the interface for abaca fiber reinforced hdpe and biope composite materials, and its influence over tensile properties. Polymers 2022;14(24):5412.

[21] Seculi F, Espinach FX, Julián F, Delgado-Aguilar M, Mutjé P, Tarrés Q. Comparative evaluation of the stiffness of abaca-fiber-reinforced bio-polyethylene and high density polyethylene composites. Polymers 2023;15(5):1096.

[22] Sia CV, Fernando L, Joseph A, Chua SN. Modified Weibull analysis on banana fiber strength prediction. J Mech Eng Sci 2018;12(1):3461–71.

[23] Trujillo E, Moesen M, Osorio L, Van Vuure AW, Ivens J, Verpoest I. Bamboo fibres for reinforcement in composite materials: strength Weibull analysis. Compos Appl Sci Manuf 2014;61:115–25.

[24] Kelly A, Tyson W. Tensile porperties of fibre-reinforced metals - copper/tungsten and copper/molybdenum. J Mech Phys Solid 1965;13(6):329–38.

[25] Monette L, Anderson MP, Grest GS. The meaning of the critical length concept in composites - study of matrix viscosity and strain rate on the average fiber fragmentation length in short-fiber polymer composites. Polym Compos 1993;14(2):101–15.

[26] Bowyer WH, Bader HG. On the reinforcement of thermoplastics by imperfectly aligned discontinuous fibres. J Mater Sci 1972;7(11). 1315-2.

[27] Beckermann GW, Pickering KL. Engineering and evaluation of hemp fibre reinforced polypropylene composites: micro-mechanics and strength prediction modelling. Compos Appl Sci Manuf 2009;40(2):210–7.

[28] Li Y, Pickering KL, Farrell RL. Determination of interfacial shear strength of white rot fungi treated hemp fibre reinforced polypropylene. Compos Sci Technol 2009;69(7–8):1165–71.

[29] Vallejos ME, Espinach FX, Julian F, Torres L, Vilaseca F, Mutje P. Micromechanics of hemp strands in polypropylene composites. Compos Sci Technol 2012;72(10):1209–13.

[30] Aliotta L, Lazzeri A. A proposal to modify the Kelly-Tyson equation to calculate the interfacial shear strength (IFSS) of composites with low aspect ratio fibers. Compos Sci Technol 2020:186.

[31] Seculi F, Espinach FX, Julian F, Delgado-Aguilar M, Mutje P, Tarres Q. Evaluation of the strength of the interface for abaca fiber reinforced hdpe and biope composite materials, and its influence over tensile properties. Polymers 2022;14(24).

[32] Li M, Pu Y, Thomas VM, Yoo CG, Ozcan S, Deng Y, et al. Recent advancements of plant-based natural fiber-reinforced composites and their applications. Compos Pt B-Eng. 2020:200.

[33] Faruk O, Bledzki AK, Fink H-P, Sain M. Biocomposites reinforced with natural fibers: 2000-2010. Prog Polym Sci 2012;37(11):1552–96.

[34] Scaffaro R, Maio A, Gulino EF, Pitarresi G. Lignocellulosic fillers and graphene nanoplatelets as hybrid reinforcement for polylactic acid: effect on mechanical properties and degradability. Compos Sci Technol 2020:190.

[35] Scaffaro R, Maio A, Gulino EF, Alaimo G, Morreale M. Green composites based on PLA and agricultural or marine waste prepared by FDM. Polymers 2021;13(9).

[36] Walker S, Rothman R. Life cycle assessment of bio-based and fossil-based plastic: a review. J Clean Prod 2020;261:121158.

[37] Granda LA, Espinach FX, Lopez F, Garcia JC, Delgado-Aguilar M, Mutje P. Semichemical fibres of Leucaena collinsii reinforced polypropylene: macromechanical and micromechanical analysis. Compos Pt B-Eng. 2016;91:384–91.

[38] Kramer RK, Felix Carvalho AJ. Non-freezing water sorbed on microcrystalline cellulose studied by high-resolution thermogravimetric analysis. Cellulose 2021;28(16):10117–25.

[39] Spiridon II. Natural fiber-polyolefin composites. MINI-REVIEW. Cellulose Chemistry and Technology 2014;48(7–8):599–611.

[40] Elgharbawy AS, Ali RM. A comprehensive review of the composites of polyolefin and their properties. Heliyon 2022:e09932.

[41] Mano B, Araújo J, Spinacé M, De Paoli M-A. Polyolefin composites with curaua fibres: effect of the processing conditions on mechanical properties, morphology and fibres dimensions. Compos Sci Technol 2010;70(1):29–35.

[42] Sobczak L, Brueggemann O, Putz RF. Polyolefin composites with natural fibers and wood-modification of the fiber/filler-matrix interaction. J Appl Polym Sci 2013; 127(1):1–17.
[43] Oliver-Ortega H, Julian F, Espinach FX, Tarrés Q, Ardanuy M, Mutjé P. Research on the use of lignocellulosic fibers reinforced bio-polyamide 11 with composites for automotive parts: car door handle case study. J Clean Prod 2019;226:64–73.
[44] Kumar R, Ul Haq MI, Raina A, Anand A. Industrial applications of natural fibre-reinforced polymer composites - challenges and opportunities. Int J Sustain Eng 2019;12(3):212–20.
[45] Delgado-Aguilar M, Tarres Q, Marques MdFV, Espinach FX, Julian F, Mutje P, et al. Explorative study on the use of curaua reinforced polypropylene composites for the automotive industry. Materials 2019;12(24).
[46] Bajwa DS, Bhattacharjee S. Current progress, trends and challenges in the application of biofiber composites by automotive industry. J Nat Fibers 2016;13 (6):660–9.
[47] Karus M, Ortmann S, Vogt D. All natural on the inside? Kunststoffe-Plast Europe. 2005;95(7):51–3.
[48] Hernández-Díaz D, Villar-Ribera R, Julián F, Tarrés Q, Espinach FX, Delgado-Aguilar M. Topography of the interfacial shear strength and the mean intrinsic tensile strength of hemp fibers as a reinforcement of polypropylene. Materials 2020;13(4):1012.
[49] Sullins T, Pillay S, Komus A, Ning H. Hemp fiber reinforced polypropylene composites: the effects of material treatments. Compos B Eng 2017;114:15–22.
[50] Johnson R. Hemp as an agricultural commodity. LIBRARY OF CONGRESS WASHINGTON DC CONGRESSIONAL RESEARCH SERVICE; 2017. p. 1–40.
[51] Pil L, Bensadoun F, Pariset J, Verpoest I. Why are designers fascinated by flax and hemp fibre composites? Compos Appl Sci Manuf 2016;83:193–205.
[52] El Messiry M. Theoretical analysis of natural fiber volume fraction of reinforced composites. Alex Eng J 2013;52(3):301–6.
[53] Shahzad A, Teacă C-A, Tanasă F. Natural fibers and surface treatment methods. In: Surface treatment methods of natural fibres and their effects on Biocomposites. Elsevier; 2022. p. 1–18.
[54] Kumar S, Manna A, Dang RJMTP. A review on applications of natural Fiber-Reinforced composites (NFRCs). Mater Today Proc 2022;50:1632–6.
[55] Reixach R, Espinach FX, Arbat G, Julián F, Delgado-Aguilar M, Puig J, et al. Tensile properties of polypropylene composites reinforced with mechanical, thermomechanical, and chemi-thermomechanical pulps from orange pruning. Bioresources 2015;10(3):4544–56.
[56] Reixach R, Franco-Marquès E, El Mansouri N-E, de Cartagena FR, Arbat G, Espinach FX, et al. Micromechanics of mechanical, thermomechanical, and chemi-thermomechanical pulp from orange tree pruning as polypropylene reinforcement: a comparative study. Bioresources 2013;8(3):3231–46.
[57] Bledzki AK, Mamun AA, Faruk O. Abaca fibre reinforced PP composites and comparison with jute and flax fibre PP composites. Express Polym Lett 2007;1(11): 755–62.
[58] Delicano JA. A review on abaca fiber reinforced composites. Compos Interfac 2018; 25(12):1039–66.
[59] Bartos A, Kocs J, Anggono J, Moczo J, Pukanszky B. Effect of fiber attrition, particle characteristics and interfacial adhesion on the properties of PP/sugarcane bagasse fiber composites. Polym Test 2021;98.
[60] Hirsch T. Modulus of elasticity of concrete affected by elastic moduli of cement paste matrix and aggregate. J Am Concr Inst 1962;59(3):427–51.
[61] Bakhori SNM, Hassan MZ, Fadzulah SHSM, Ahmad F. Tensile properties of Jute-polypropylene composites. J Chemical Engineering Transactions 2018;63:727–32.
[62] Ariawan D, Smaradhana DF, Akbar HI. Micromechanical analysis of elastic modulus and tensile strength on randomised discontinuous alkali and heat treated kenaf fiber—unsaturated polyester composites. In: Proceedings of the 6th International Conference and Exhibition on sustainable Energy and Advanced materials: ICE-SEAM 2019, 16—17 October 2019. Surakarta, Indonesia: Springer; 2020. p. 1–12.
[63] Cao Y, Wang W, Wang Q, Wang H. Application of mechanical models to flax fiber/wood fiber/plastic composites. J BioResources 2013;8(3):3276–88.
[64] Salem S, Oliver-Ortega H, Espinach FX, Hamed KB, Nasri N, Alcalà M, et al. Study on the tensile strength and micromechanical analysis of alfa fibers reinforced high density polyethylene composites. Fibers Polym 2019;20(3):602–10.
[65] Fu SY, Lauke B. Effects of fiber length and fiber orientation distributions on the tensile strength of short-fiber-reinforced polymers. Compos Sci Technol 1996;56 (10):1179–90.
[66] Delgado Aguilar M, Julián Pérez F, Pèlach Serra MÀ, Espinach Orús X, Méndez González JA, Mutjé Pujol P. Fast and simple method for prediction of the micromechanical parameters and macromechanical properties of composite materials. © Cellulose Chemistry and Technology 2016;50(3–4):423–8. 2016.